Guidance, Navigation, and Control and Co-located Conferences
August 19-22, 2013, Boston, MA
AIAA Guidance, Navigation, and Control (GNC) Conference

Nonlinear Adaptive Output Feedback Control of Flexible-Joint Space Robot Manipulators

Steve Ulrich[1] and Jurek Z. Sasiadek[2]
Carleton University, Ottawa, Ontario, K1S 5B6, Canada

and

Itzhak Barkana[3]
Barkana Consulting, 47209 Ramat-Hasharon, Israel

Growing research interest in space robotic systems capable of accurately performing autonomous manipulation tasks within an acceptable execution time has led to an increased demand for lightweight materials and mechanisms. As a result, joint flexibility effects become important, and represent the main limitation to achieving satisfactory trajectory tracking performance. This paper addresses the nonlinear adaptive output feedback control problem for flexible-joint space manipulators. Composite control schemes in which decentralized simple adaptive control-based adaptation mechanisms to control the quasi-steady state robot subsystem are added to a linear correction term to stabilize the boundary layer subsystem, are proposed. An almost strictly passivity-based approach is adopted to guarantee closed-loop stability of the quasi-steady state subsystem. Simulation results are included to highlight the performance and robustness to parametric uncertainties and modeling errors of the proposed composite control methodologies.

I. Introduction

Upcoming space robot manipulators, such as the Next-Generation Canadarm developed jointly by Macdonald Detwiller and Associates and the Canadian Space Agency, are expected to be built of slender aluminum-composite links, whose structural flexibility will be greater than that of their predecessors. Moreover, the latest generation of advanced space robots specifically designed for on-orbit servicing operations are equipped with extremely lightweight joint mechanisms, including harmonic drives. These gear mechanisms have received increasing attention in robotic applications due to their attractive properties such as high reduction ratio, compact size, low weight, and coaxial assembly. However, with harmonic drives, elastic vibrations of the flexspline are the main issue that significantly challenges control system development. As explained by Sweet and Good,[1] joint stiffness coupled with damping at the joints can lead to strongly resonant behaviors when using rigid control schemes, unless the control bandwidth is severely restricted. In addition, when handling large payloads, joint or structural flexibility effect become even more important and can result in payload-attitude controller fuel-replenishing dynamic interactions. Although both joint and link flexibility effects are important for space manipulators, joint flexibility is often considered more important than link flexibility, at least in the operational range of space robot manipulator.[2]

Despite the considerable research work that has been done on the dynamics and control of flexible-joint robot manipulators, the topic remains an important area of contemporary research, as noted by Ozgoli and Taghirad,[3] and several constraints and limitations are yet to be overcome. Indeed, most existing flexible-joint control strategies reported in the literature (e.g. nonlinear backstepping control,[4] feedback linearization,[5] optimal control,[6] and robust control[7]) are model-based techniques, and have reasonably good tracking performance only when substantial knowledge of the plant mathematical model and its parameters is available. Consequently, if significant or

[1]PhD Candidate, Department of Mechanical and Aerospace Engineering, 1125 Colonel By Drive; now Assistant Professor, Member AIAA.
[2]Professor, Department of Mechanical and Aerospace Engineering, 1125 Colonel By Drive, Associate Fellow AIAA.
[3]President, 11 Hashomer Street, Associate Fellow AIAA.

unpredictable plant parameter variations arise as a result of joint mechanism degradation, or if there are modeling errors due to complex flexible dynamics behaviors, model-based control approaches might perform inadequately. In this context, this paper considers the adaptive trajectory tracking problem associated with flexible-joint space manipulators subject to uncertainties.

References 8 and 9 consider composite direct adaptive control of flexible-joint manipulators mounted on a stationary spacecraft using a simple adaptive control-based gain adaptation mechanism and a fuzzy logic adaptation law, respectively. Although these previous work report satisfactory trajectory tracking results with good robustness properties to both parametric uncertainties and dynamics modeling errors, no guarantees of closed-loop stability are provided.

Similarly to Refs. 8 and 9, this paper is concerned with composite adaptive control of flexible-joint space robot manipulators subject to parametric uncertainties and dynamics modeling errors. The proposed controllers are composed of a direct adaptive output feedback slow control term that controls the quasi-steady state subsystem, and a linear fast control term which controls the boundary-layer subsystem. Based on recent theoretical developments on stable direct adaptive control algorithms for nonlinear square systems,[10,11] slow control terms employing the decentralized simple adaptive control (DSAC), and the decentralized modified simple adaptive control (DMSAC) techniques are proposed. These two design approaches use the almost strictly passive (ASP) conditions for nonlinear systems,[12] to guarantee closed-loop convergence of the slow output feedback adaptive control term. Invoking Tychonov's theorem, both composite controllers ensure that the tracking errors do not deviate more than of the order $O(\epsilon)$ from the its quasi-steady state on a finite time interval, where ϵ is a small positive scalar which is inversely proportional to the joint stiffness matrix.

Unlike existing composite adaptive controllers for flexible-joint robots, the proposed design is an output feedback approach that does not require identification of unknown parameters or mathematical models of the system to be controlled. Specifically, both adaptive controller design proposed in this paper are based on the Model Reference Adaptive Control (MRAC) approach and deal with modeling errors and parameter uncertainties by time-varying the controllers' gains using computationally efficient adaptation laws, in order to reduce the errors between an ideal model and the actual robot system.

After reviewing flexible-joint space manipulators dynamics and kinematics, preliminary definitions are given, and a theorem that defines under which conditions a nonlinear square system is ASP is reported. The proposed composite adaptive output feedback control designs are then discussed, first showing that the quasi-steady state subsystem model of a flexible-joint space robot manipulator with an end-effector Cartesian scaled-position-plus-velocity output feedback is ASP. A DSAC and a DMSAC control design for the boundary-layer model are then proposed. It is then shown that these two adaptive controllers can be coupled to a simple linear correction term for the boundary-layer model, to guarantee the stability of the resulting composite controllers. Finally, numerical examples and closing remarks are given.

II. Robot Dynamics and Kinematics

In this section, the dynamics model of an *n*-link flexible-joint space manipulator is obtained using the Euler-Lagrange formulation. Since the time scale of robotic motions are assumed to be relatively small compared to the orbital period, orbital mechanics effects are neglected. Assuming lumped flexibility at the joints, links are considered rigid and the kinetic energy of the system is obtained as the summation of the kinetic energy of the links, denoted by $T_r \in \mathbb{R}$, and of the kinetic energy of the rotors, denoted by $T_e \in \mathbb{R}$, as follows

$$T = T_r + T_e \tag{1}$$

where T_r is obtained by the following quadratic expression

$$T_r = \frac{1}{2}\sum_{i=1}^{n}\sum_{j=1}^{n} M_{ij}\dot{q}_i\dot{q}_j = \frac{1}{2}\dot{q}^T M(q)\dot{q} \tag{2}$$

where $M(q) \in \mathbb{R}^{n\times n}$ denotes the positive-definite link inertia matrix, and $q \in \mathbb{R}^n$ denotes the link angles. The kinetic energy of the rotors is assumed to be due to the rotor rotation only, and is given by

$$T_e = \frac{1}{2}\sum_{i=1}^{n}\sum_{j=1}^{n} J_{m_{ij}}\dot{q}_{m_i}\dot{q}_{m_j} = \frac{1}{2}\dot{q}_m^T J_m \dot{q}_m \tag{3}$$

where $J_m \in \mathbb{R}^{n\times n}$ denotes the positive-definite motor inertia matrix, $q_m \in \mathbb{R}^n$ denotes the motor angles. For space-based robots, microgravity effects are very small compared to control input forces, and hence, can be neglected. Thus, the potential energy, denoted by $U \in \mathbb{R}$, is only due to joint elasticity, as follows

$$U = \frac{1}{2}\sum_{i=1}^{n}\sum_{j=1}^{n} k_{ij}\left(q_i - q_{m_i}\right)\left(q_j - q_{m_j}\right) = \frac{1}{2}\left(q - q_m\right)^T k\left(q - q_m\right) \tag{4}$$

where $k \in \mathbb{R}^{n\times n}$ is the joint stiffness matrix which be defined as $k = k_1/\varepsilon^2$, with $k_1 \in \mathbb{R}^{n\times n}$ and with $\varepsilon \in \mathbb{R}$ as a small positive parameter. The nonlinear dynamics equations of motion a manipulator subjected to a generalized force τ_i acting on the generalized coordinates q_i, are obtained by

$$\tau_i = \frac{d}{dt}\left(\frac{\partial L}{\partial \dot{q}_i}\right) - \frac{\partial L}{\partial q_i} \tag{5}$$

where $L \in \mathbb{R}$ denotes the Lagrangian

$$L(q_i, \dot{q}_i) = T - U \tag{6}$$

Thus, the Euler-Lagrange dynamics equations of motion of a n-DOF flexible-joint space manipulator mounted on a stationary spacecraft, with revolute joints and actuated directly by DC motors is given by[13]

$$M(q)\ddot{q} + C(q,\dot{q})\dot{q} - k(q_m - q) = 0 \tag{7}$$

$$J_m\ddot{q}_m + k(q_m - q) = \tau \tag{8}$$

where the definition of $M(q)$ and $C(q,\dot{q})$ for a two-link manipulator can be found in Ref. 14. The control input torque is denoted by $\tau \in \mathbb{R}^2$ and will be distributed between a slow control torque τ_s and a fast control torque τ_f. Following common flexible-joint controller design practice, the singular perturbation-based theory is employed, to provide a framework for the design of composite controllers, in which the motor torque control input τ is composed of a slow control term τ_s and a fast control term τ_f

$$\tau = \tau_s + \tau_f \tag{9}$$

where subscript *s* stands for slow variables defined in the slow time scale *t*, and the subscript *f* stands for variables defined in the fast time scale t/ε. The slow control term is designed to stabilize the quasi-steady-state model (slow subsystem), whereas the fast-control torque is applied to the boundary-layer model (fast subsystem).

In the following, it is assumed that the two-link robot manipulator system defined in Eqs. (7) and (8) is fully-actuated and non-redundant, and that the Jacobian matrix denoted by $J(q) \in \mathbb{R}^{2\times 2}$ has full rank column. Thus, holonomic constraints can be selected in order for the actual Cartesian velocity vector, denoted $\dot{x}_r \in \mathbb{R}^2$ to satisfy the relation

$$\dot{x}_r = J(q)\dot{q} \tag{10}$$

Similarly, it is assumed that there exists a mapping allowing the Cartesian end-effector position vector, denoted $x_r \in \mathbb{R}^2$ with respect to the robot reference frame along both axes to be obtained as

$$x_r = \Omega(q) \tag{11}$$

where $\Omega(q) \in \mathbb{R}^2$ is the nonlinear forward kinematic transforming the link positions into end-effector Cartesian position. Assuming that the robot manipulator is equipped with joint encoders and tachometers, Eqs. (10) and (11) can be combined to map joint-space variables into a task-space (Cartesian) vector, denoted $x \in \mathbb{R}^4$, through the nonlinear transformation[14]

$$x \equiv \begin{bmatrix} x_r \\ \dot{x}_r \end{bmatrix} = \begin{bmatrix} l_1 \cos(q_1) + l_2 \cos(q_1 + q_2) \\ l_1 \sin(q_1) + l_2 \sin(q_1 + q_2) \\ -l_1 \sin(q_1)\dot{q}_1 - l_2 \sin(q_1 + q_2)(\dot{q}_1 + \dot{q}_2) \\ l_1 \cos(q_1)\dot{q}_1 + l_2 \cos(q_1 + q_2)(\dot{q}_1 + \dot{q}_2) \end{bmatrix} \tag{12}$$

The scaled-position-plus-velocity output vector of the robot manipulator, denoted $y \in \mathbb{R}^2$ is then formed as

$$y = \alpha x_r + \dot{x}_r \tag{13}$$

where $\alpha \in \mathbb{R}$ is a known positive-definite scaling gain.

III. Almost Strictly Passive Nonlinear Systems

Consider a class of nonlinear square systems described by the following state-space transformation formulation

$$\dot{x}(t) = A(x,t)x(t) + B(x,t)u(t) \tag{14a}$$

$$y(t) = Cu(t) \tag{14a}$$

where

$$x = \begin{bmatrix} x_1 \\ \vdots \\ x_n \end{bmatrix} \in \mathbb{R}^n, \quad u = \begin{bmatrix} u_1 \\ \vdots \\ u_m \end{bmatrix} \in \mathbb{R}^m, \quad y = \begin{bmatrix} y_1 \\ \vdots \\ y_m \end{bmatrix} \in \mathbb{R}^m$$

are the system states, inputs and outputs, respectively, and A, B, and C are appropriately dimensioned real matrices. For completeness, the following definitions and the ASP theorem applicable to the system specified by Eq. (14) are presented below. For a more detailed treatment on these definitions and theorem, the reader is referred to Ref. 12.

Definition 3.1: The nonlinear system described by Eq. (14) is uniformly strictly minimum-phase if its zero-dynamics is uniformly stable. In other words, there exist two matrices $M(x,t)$ and $N(x,t)$ satisfying the following relations

$$CM = 0 \tag{15a}$$

$$NB = 0 \tag{15b}$$

$$NM = I_m \tag{15c}$$

such that the resulting zero dynamics given by

$$\dot{z} = \left(\dot{N} + NA\right)Mz \tag{16}$$

is uniformly asymptotically stable. In Eq. (15c), I_m denotes the $m \times m$ identity matrix.

Definition 3.2: The nonlinear system described by Eq. (14) is strictly passive (SP) if there exist two positive definite symmetric (PDS) matrices $P(x,t)$ and $Q(x,t)$ such that the following two conditions are simultaneously satisfied

$$\dot{P} + PA + A^T P = -Q \tag{17a}$$

$$PB = C^T \tag{17b}$$

The Lyapunov differential equation (17a) shows that a SP system is uniformly asymptotically stable, whereas the second relation (17b) shows that

$$B^T PB = B^T C^T = \left(CB\right)^T = CB \tag{18}$$

which implies that the product CB is PDS. As most real-world systems are not inherently SP, a class of almost strictly passive (ASP) systems can be defined through definition 3.

Definition 3.3: The nonlinear system described by Eq. (14) is ASP if there exist two PDS matrices $P(x,t)$ and $Q(x,t)$ and a constant output feedback gain $\tilde{K}_e$ such that the closed-loop system

$$\dot{x}(t) = \left[A - B\tilde{K}_e C\right]x(t) \tag{19a}$$

$$y(t) = Cx(t) \tag{19b}$$

simultaneously satisfies the following ASP relations

$$\dot{P} + P(A - B\tilde{K}_e C) + (A - B\tilde{K}_e C)^T P = -Q \tag{20a}$$

$$PB = C^T \tag{20b}$$

Theorem 3.1: Any uniformly strictly minimum-phase nonlinear systems described by described by Eq. (14), with the product CB being PDS is ASP.

IV. Control Objective

The control objective consists in ensuring that the nonlinear flexible-joint manipulator system tracks the output vector $y_m(t)$ of a (not necessarily square) ideal model

$$\dot{x}_m(t) = A_m x_m(t) + B_m u_m(t) \tag{21a}$$

$$y_m(t) = C_m x_m(t) \tag{21b}$$

where

$$x_m = \begin{bmatrix} x_{m_1} \\ \vdots \\ x_{m_{n_m}} \end{bmatrix} \in \mathbb{R}^{n_m}, \quad u_m = \begin{bmatrix} u_{m_1} \\ \vdots \\ u_{m_{p_m}} \end{bmatrix} \in \mathbb{R}^{p_m}, \quad y_m = \begin{bmatrix} y_{m_1} \\ \vdots \\ y_{m_m} \end{bmatrix} \in \mathbb{R}^m$$

are the ideal model states, inputs and outputs, respectively, and A_m, B_m, and C_m are appropriately dimensioned real matrices. It is assumed that both n_m and p_m are multiples of *m*. In other words, $n_m = km$ and $p_m = lm$ where $k, l \in \mathbb{R}$ are positive scalars. To quantify the control objective, an output error, denoted by $e_y(t) \in \mathbb{R}^m$, is defined as

$$e_y \triangleq y_m - y \tag{22}$$

When the system tracks the ideal model perfectly, i.e. $y_m = y^* = Cx^*$, it moves along some bounded *ideal* state trajectory denoted $x^*(t) \in \mathbb{R}^n$. To facilitate the subsequent analysis, a state error, denoted by $e_x(t) \in \mathbb{R}^n$, is defined as

$$e_x \triangleq x^* - x \tag{23}$$

Thus, Eq. (22) can be rewritten as

$$e_y = Cx^* - Cx = Ce_x \tag{24}$$

It is assumed that both n_m and p_m are multiples of *m*. In other words, $n_m = km$ and $p_m = lm$ where $k, l \in \mathbb{R}$ are positive scalars.

V. Adaptive Output Feedback Control of the Quasi-Steady State Model

This section first presents a theorem that ensures that the quasi-steady state model of a flexible-joint manipulator with a scaled-position-plus-velocity output matrix is ASP. Then, two direct adaptive control laws for this ASP subsystem are developed, and finally, the stability analysis of the resulting closed-loop subsystems is discussed.

A. Almost Strictly Passive (ASP) Property

The quasi-steady state model of a two-link flexible-joint manipulator, which has a form equivalent to the rigid-joint dynamics model, is given by

$$H(q_s)\ddot{q}_s + C(q_s, \dot{q}_s)\dot{q}_s = \tau_s \tag{25}$$

where

$$H(q_s) = M(q_s) + J_m \tag{26}$$

where the subscript *s* denotes variables defined at $\epsilon = 0$. Let rewrite the joint-space dynamics of quasi-steady state model defined by Eq. (25) into the task space dynamics, as follows

$$\Lambda(q_s)\ddot{x}_{p_s} + \Pi(q_s, \dot{q}_s)\dot{x}_{p_s} = f_s \tag{27}$$

where $\Lambda(q_s)$, $\Pi(q_s, \dot{q}_s) \in \mathbb{R}^{2\times 2}$ and $f_s \in \mathbb{R}^2$ denote the pseudo-inertia and Coriolis/centrifugal matrices, and force vector, which are respectively given by

$$\Lambda(q_s) = J^{-T}(q)M(q)J^{-1}(q) \tag{28a}$$

$$\Pi(q_s, \dot{q}_s) = J^{-T}(q)C(q,\dot{q})J^{-1}(q) + \Lambda(q)J(q)\dot{J}^{-1}(q) \tag{28b}$$

$$f_s = J^{-T}(q)\tau_s \tag{28c}$$

Theorem 5.1: The quasi-steady state model of a flexible-joint manipulator expressed in the task space by Eq. (27) with a scaled-position-plus-velocity output matrix is ASP.

Proof: The nonlinear system dynamics can be expressed in a standard state-space representation, with matrices given by

$$A = \begin{bmatrix} 0 & I_2 \\ 0 & -\Lambda^{-1}(q_s)\Pi(q_s,\dot{q}_s) \end{bmatrix} \qquad B = \begin{bmatrix} 0 \\ \Lambda^{-1}(q_s) \end{bmatrix} \qquad C = \begin{bmatrix} \alpha I_2 & I_2 \end{bmatrix}$$

where the state vector is defined in Eq. (12) and where $u = f_s$. Thus, is can be seen that the product CB is PDS

$$CB = \begin{bmatrix} \alpha I_2 & I_2 \end{bmatrix} \begin{bmatrix} 0 \\ \Lambda^{-1}(q_s) \end{bmatrix} = \Lambda^{-1}(q_s) > 0 \tag{29}$$

Moreover, a simple selection of matrices that satisfies Eq. (15) is

$$M = \begin{bmatrix} I_2 \\ -\alpha I_2 \end{bmatrix} \qquad N = \begin{bmatrix} I_2 & 0 \end{bmatrix} \tag{30}$$

The A_z matrix is therefore given by

$$A_z = NAM = -\alpha I_2 \tag{31}$$

Thus resulting in a zero dynamics equation of the form

$$\dot{z} = A_z z = -\alpha z \tag{32}$$

which shows that the zero dynamics is stable and that the nonlinear dynamics of the quasi-steady state model is uniformly minimum-phase. Invoking *Theorem 3.1* completes the proof.

B. Adaptive Control Laws

Given that the quasi-steady state model of a flexible-joint manipulator which employs a scaled-position-plus-velocity feedback is ASP, stability of the quasi-steady state model can be guaranteed by using either the decentralized simple adaptive control (DSAC) or the decentralized modified simple adaptive control (DMSAC) techniques.[10,11]

1. *Decentralized Simple Adaptive Control*

The standard SAC algorithm is adopted as the slow control term[15]

$$u = K_e(t)e_y + K_x(t)x_m + K_u(t)u_m \tag{33}$$

where $K_e(t) \in \mathbb{R}^{m\times m}$ is the time-varying stabilizing control gain matrix, and $K_x(t) \in \mathbb{R}^{m\times n_m}$ and $K_u(t) \in \mathbb{R}^{m\times p_m}$ are time-varying feedforward control gain matrices that contribute to maintaining the stability of the controlled

system, and to bringing the output tracking error to zero. Each control gain matrix is calculated as the summation of a proportional and an integral component, as follows

$$K_e(t) = K_{Pe}(t) + K_{Ie}(t) \tag{34}$$

$$K_x(t) = K_{Px}(t) + K_{Ix}(t) \tag{35}$$

$$K_u(t) = K_{Pu}(t) + K_{Iu}(t) \tag{36}$$

where only the integral adaptive control terms are absolutely necessary to guarantee the stability of the direct adaptive control system. However, including the proportional adaptive control terms increases the rate of convergence of the adaptive system toward perfect tracking.

Using the DSAC adaptation mechanism,[10,11] the proportional and the integral components of the stabilizing control gain in Eq. (33), $K_{Pe}(t)$, $K_{Ie}(t) \in \mathbb{R}^{m\times m}$ are both updated by the output tracking error only, which results in the following adaptation law

$$K_{Pe}(t) = \text{diag}\left\{e_y e_y^T\right\}\Gamma_{Pe} \tag{37a}$$

$$\dot{K}_{Ie}(t) = \text{diag}\left\{e_y e_y^T\right\}\Gamma_{Ie} \tag{37b}$$

The components of the feedforward gain matrices $K_{Px}(t)$, $K_{Ix}(t) \in \mathbb{R}^{m\times n_m}$, and $K_{Pu}(t)$, $K_{Iu}(t) \in \mathbb{R}^{m\times p_m}$ are updated in a similar fashion, as follows:

$$K_{Px}(t) = R^T \text{diag}\left\{R e_y x_m^T\right\}\Gamma_{Px} \tag{38a}$$

$$\dot{K}_{Ix}(t) = R^T \text{diag}\left\{R e_y x_m^T\right\}\Gamma_{Ix} \tag{38b}$$

$$K_{Pu}(t) = T^T \text{diag}\left\{T e_y u_m^T\right\}\Gamma_{Pu} \tag{38c}$$

$$\dot{K}_{Iu}(t) = T^T \text{diag}\left\{T e_y u_m^T\right\}\Gamma_{Iu} \tag{38d}$$

where

$$R = \begin{bmatrix} I_m \\ I_m \\ \vdots \\ I_m \end{bmatrix} \in \mathbb{R}^{n_m\times m}, \qquad T = \begin{bmatrix} I_m \\ I_m \\ \vdots \\ I_m \end{bmatrix} \in \mathbb{R}^{p_m\times m}$$

and where Γ_{Pe}, $\Gamma_{Ie} \in \mathbb{R}^{m\times m}$, Γ_{Px}, $\Gamma_{Ix} \in \mathbb{R}^{n_m\times n_m}$ and Γ_{Pu}, $\Gamma_{Iu} \in \mathbb{R}^{p_m\times p_m}$ are constant diagonal matrices that control the rate of adaptation.

The adaptive algorithm can be rewritten in the following concise form

$$u = K(t)\, r \tag{39}$$

where $K(t) \in \mathbb{R}^{m\times(m+n_m+p_m)}$ and $r \in \mathbb{R}^{(m+n_m+p_m)\times m}$ are respectively defined as

$$K(t) = \begin{bmatrix} K_e(t) & K_x(t) & K_u(t) \end{bmatrix} = K_P(t) + K_I(t) \tag{40}$$

$$r = \begin{bmatrix} e_y^T & x_m^T & u_m^T \end{bmatrix}^T \tag{41}$$

With this representation, $K_P(t)$, $K_I(t) \in \mathbb{R}^{m\times(m+n_m+p_m)}$ are updated as follows

$$K_P(t) = S^T \operatorname{diag}\left\{Se_y r^T\right\}\Gamma_P \tag{42a}$$

$$\dot{K}_I(t) = S^T \operatorname{diag}\left\{Se_y r^T\right\}\Gamma_I \tag{42b}$$

where Γ_P , $\Gamma_I \in \mathbb{R}^{(m+n_m+p_m)\times(m+n_m+p_m)}$ and where the scaling matrix S is given by $\mathbb{R}^{(m+n_m+p_m)\times(m+n_m+p_m)}$

$$S = \begin{bmatrix} I_m \\ I_m \\ \vdots \\ I_m \end{bmatrix} \in \mathbb{R}^{(m+n_m+p_m)\times m}$$

Time-differentiating Eq. (23), and after some algebra, gives the following differential equation of the state error

$$\dot{e}_x = \left(A - B\tilde{K}_e C\right)e_x + \left(A^* - A\right)x^* + \left(B^* - B\right)u^* - BK_P(t)r - B\left(K_I(t) - \tilde{K}\right)r \tag{43}$$

where $\tilde{K}_e$ is any stabilizing control gain, and where $\tilde{K}$ is defined as

$$\tilde{K} = \begin{bmatrix} \tilde{K}_e & \tilde{K}_x & \tilde{K}_u \end{bmatrix} \tag{44}$$

where $\tilde{K}_x, \tilde{K}_u$ denote the ideal feedforward control gains. When the control is such that perfect tracking occurs, the output tracking error is

$$e_y = y_m - y = 0 \tag{45}$$

In this case, the ideal control input τ_s^* is given by

$$u^* = \tilde{K}_x x_m + \tilde{K}_u u_m \tag{46}$$

2. Decentralized Modified Simple Adaptive Control

To decrease the computational power required to implement the adaptive control algorithm, the modified SAC (MSAC) idea can be used.[16] With MSAC, as opposed to SAC, the control law is obtained by retaining only the error-related adaptive control gain $K_e(t)$ in Eq. (33). In fact, as mentioned in Ref. 17, only the stabilizing control gain matrix $K_e(t)$ is absolutely required for the stability of the adaptive control methodology. Adopting the MSAC approach to compute the slow control torque yields the following control law

$$u = K_e(t)e_y = \left[K_{Pe}(t) + K_{Ie}(t)\right]e_y \tag{47}$$

where $K_{Pe}(t)$ and $K_{Ie}(t)$ are updated with the decentralized adaptation law given in Eq. (37).

With the resulting DMSAC methodology, the ideal control input is zero, since $e_y = 0$ along the ideal trajectory. In this case, the differential equation of the state error becomes

$$\dot{e}_x = \left(A - B\tilde{K}_e C\right)e_x + \left(A^* - A\right)x^* - BK_{Pe}(t)e_y - B\left(K_{Ie}(t) - \tilde{K}_e\right)e_y \tag{48}$$

C. Brief Review of Stability

To show the asymptotic convergence of the tracking errors and that the adaptive gains are bounded, the proof of stability must considers the adaptive system defined by both Eqs. (42b) and (43), and Eqs. (37b) and (48), for DSAC and DMSAC, respectively.

1. Decentralized Simple Adaptive Control

Choosing a continuously-differentiable positive-definite quadratic Lyapunov function of the form

$$V = e_x^T P e_x + \mathrm{tr}\left[\left(K_I(t) - \tilde{K}\right)\Gamma_I^{-1}\left(K_I(t) - \tilde{K}\right)^T\right] \tag{49}$$

and using the ASP relations given by Eq. (20) results in the following time-derivative of the Lyapunov function

$$\dot{V} = -e_x^T Q e_x - 2e_x^T C^T S^T \mathrm{diag}\left\{SCe_x r^T\right\}\Gamma_P r \tag{50}$$

The Lyapunov function (49) is positive-definite quadratic in terms of all state variables of the dynamical system $\left\{e_x, K_I(t)\right\}$. The Lyapunov derivative (50) however, only includes the state error e_x and is therefore negative-definite in e_x and negative-semidefinite in the state-gain space $\left\{e_x, K_I(t)\right\}$. Stability of the adaptive system is therefore guaranteed from Lyapunov stability theory, and all state errors (and output errors), as well as adaptive control gains are bounded. Furthermore, LaSalle's invariance principle for non-autonomous systems[12,15,18,19] can be used to demonstrate the asymptotic stability of the tracking errors.

The well-known σ terms[20] can be included in the gain adaptation mechanism to ensure that the integral adaptive control gains remain bounded in cases where the tracking error would not reach zero. With this adjustment, the time-varying integral control gains are obtained as follows

$$\dot{K}_{Ie}(t) = \mathrm{diag}\left\{e_y e_y^T\right\}\Gamma_{Ie} - \sigma_e K_{Ie}(t) \tag{51a}$$

$$\dot{K}_{Ix}(t) = R^T\left(\mathrm{diag}\left\{Re_y x_m^T\right\}\Gamma_{Ix} - \mathrm{diag}\left\{\sigma_x R K_{Ix}(t)\right\}\right) \tag{51b}$$

$$\dot{K}_{Iu}(t) = T^T\left(\mathrm{diag}\left\{Te_y u_m^T\right\}\Gamma_{Iu} - \mathrm{diag}\left\{\sigma_u T K_{Iu}(t)\right\}\right) \tag{51c}$$

and similarly,

$$\dot{K}_I(t) = S^T\left(\mathrm{diag}\left\{Se_y r^T\right\}\Gamma_I - \mathrm{diag}\left\{\sigma_I S K_I(t)\right\}\right) \tag{52}$$

where $\sigma_e \in \mathbb{R}^{m\times m}$, $\sigma_x \in \mathbb{R}^{n_m\times n_m}$, $\sigma_u \in \mathbb{R}^{p_m\times p_m}$, and $\sigma_I \in \mathbb{R}^{(m+n_m+p_m)\times(m+n_m+p_m)}$ denote the forgetting coefficient matrices. With this modification to the DSAC algorithm, the derivative of the Lyapunov function Eq. (49) becomes

$$\dot{V} = -e_x^T Q e_x - 2e_x^T C^T S^T \mathrm{diag}\left\{SCe_x r^T\right\}\Gamma_P r - 2\mathrm{tr}\left[\mathrm{S}^{\mathrm{T}}\mathrm{diag}\left\{\sigma_I S K_I(t)\right\}\Gamma_I^{-1}\left(K_I(t) - \tilde{K}\right)^T\right] \tag{53}$$

Thus, according to Lyapunov-LaSalle theorem, the application of the DSAC algorithm with the forgetting terms results in bounded error tracking. Note that, although it affects the proof of stability, the use of the DSAC control law with this adjustment is preferable in most practical applications. Without the forgetting terms, the integral adaptive gains are allowed to increase for as long as there is a tracking error. When the integral gains reach certain

values, they have a stabilizing effect on the system and the tracking error begins to decrease. However, if the tracking error does not reach zero for some reasons, the integral gains will continue to increase and eventually diverge. On the other hand, with the forgetting terms the integral gains increase as required (e.g. due to large tracking errors), and decrease when large gains are no longer necessary. In fact, with the forgetting terms, the integral gains are obtained as a first-order filtering of the tracking errors, and cannot diverge unless the tracking errors diverge.

2. Decentralized Modified Simple Adaptive Control

Choosing a continuously-differentiable positive-definite quadratic Lyapunov function of the form

$$V = e_x^T P e_x + \mathrm{tr}\left[\left(K_{Ie}(t) - \tilde{K}_e\right)\Gamma_{Ie}^{-1}\left(K_{Ie}(t) - \tilde{K}_e\right)^T \right] \tag{54}$$

and using the ASP relations given by Eq. (20) results in the following time-derivative of the Lyapunov function

$$\dot{V} = -e_x^T Q e_x - 2e_x^T C^T \mathrm{diag}\left\{Ce_x e_x^T C^T\right\}\Gamma_{Pe} Ce_x \tag{55}$$

By considering σ_e in the algorithm, $K_{Ie}(t)$ is obtained with Eq. (51a), and the Lyapunov derivative becomes

$$\dot{V} = -e_x^T Q e_x - 2e_x^T C^T \mathrm{diag}\left\{Ce_x e_x^T C^T\right\}\Gamma_{Pe} Ce_x - 2\mathrm{tr}\left[\sigma_e K_{Ie}(t)\Gamma_{Ie}^{-1}\left(K_{Ie}(t) - \tilde{K}_e\right)^T \right] \tag{56}$$

and the same conclusion about stability than that the DSAC algorithm can be drawn.

VI. Composite Control Laws

As explained earlier, the motor torque control input τ is composed of a slow control term τ_s and a fast control term τ_f. To guarantee closed-loop stability of the entire flexible system, Tychonov's theorem[21] states that the fast control term must guarantees the exponential stability of the closed-loop boundary-layer subsystem, and that the slow control term must guarantees convergence of the tracking error for the closed-loop quasi-steady state subsystem. Doing so will ensure that the tracking error will not deviate more than of the order $O(\varepsilon)$ from its quasi-steady state on a finite time interval. Thus, the smaller ε is, the greater the tracking accuracy. From the definition of k given in Sec. II, it can be concluded that better tracking results are achieved when the joint stiffness matrix is greater; in other words, when the boundary-layer is considerably faster than the quasi-steady state subsystem. Since the convergence of the closed-loop quasi-steady state subsystem was demonstrated in Sec. V, all that remains is to select an exponentially stable fast control term.

Given that the boundary-layer subsystem is LTI, a simple linear correction of the form

$$\tau_f = K_v(\dot{q} - \dot{q}_m) \tag{57}$$

is sufficient to ensure exponential stability of the boundary layer subsystem,[22] where $K_v \in \mathbb{R}^{2\times 2}$ is a constant diagonal control gain that provides additional damping of the elastic vibrations at the joints. Combining Eqs. (33) and (47) to Eq. (57), and making use of Eq. (28c), results in the following DSAC and DMSAC-based composite control law

$$\tau = J^T(q)\left[K_e(t)e_y + K_x(t)x_m + K_u(t)u_m\right] + K_v(\dot{q} - \dot{q}_m) \tag{58}$$

$$\tau = J^T(q)K_e(t)e_y + K_v(\dot{q} - \dot{q}_m) \tag{59}$$

The resulting control strategy block diagrams are provided in Figs. 1 and 2, respectively.

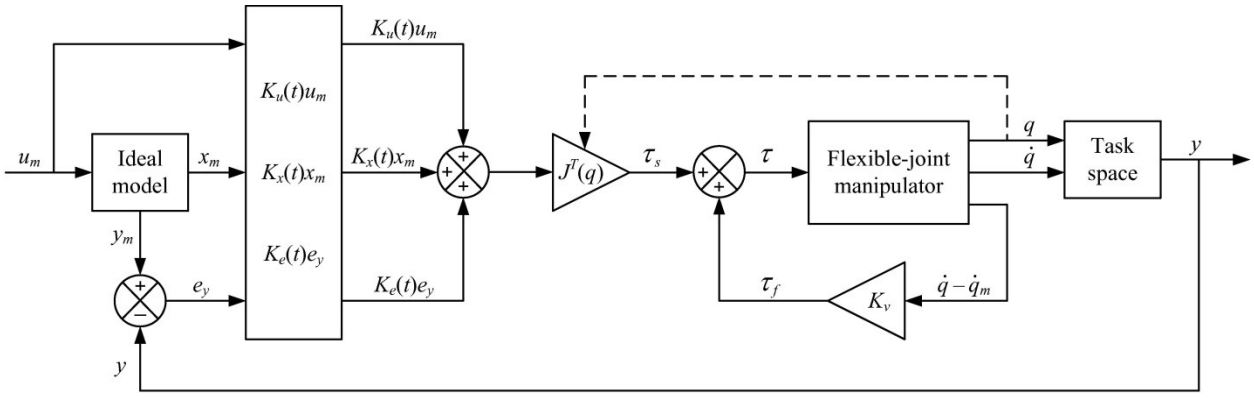

Fig. 1 Block diagram representation of the DSAC-based composite controller.

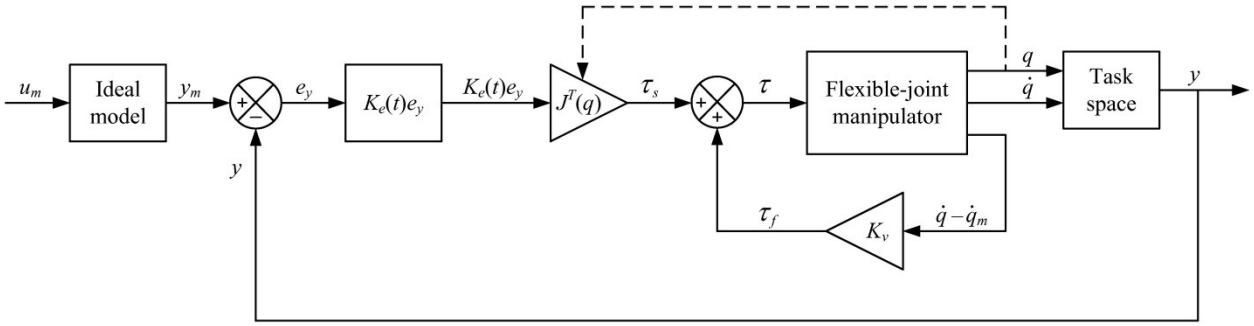

Fig. 2 Block diagram representation of the DMSAC-based composite controller.

VII. Numerical Simulation Results

To validate the nominal trajectory tracking performance, the control strategies were applied to the linear joint stiffness robot manipulator described in Sec. II. Although Readman[23] suggests joint stiffness values on the order of 10^4 N·m/rad for a harmonic drive joint, and 10^3 N·m/rad for a flexible coupling joint, the joint parameters are based on Cao and de Silva,[24] which are representative of manipulators with obvious flexible effects in their joints. The parameters of the two-link flexible joint manipulator were thus selected as: $l_1 = l_2 = 4.5$ m, $m_1 = m_2 = 1.5075$ kg, $J_{m1} = J_{m2} = 1$ kg·m^2, $k_1 = k_2 = 500$ N·m/rad, and $\alpha = 0.5$. In this work, the ideal model was designed to incorporate the desired input-output plant behavior, which is expressed in terms of the ideal damping ratio $\zeta \in \mathbb{R}$ and undamped natural frequency $\omega_n \in \mathbb{R}$, as follows

$$A_m = \begin{bmatrix} 0 & 0 & 0 & 0 \\ 0 & 0 & 0 & 0 \\ -\omega_n^2 & 0 & -2\zeta\omega_n & 0 \\ 0 & -\omega_n^2 & 0 & -2\zeta\omega_n \end{bmatrix}, \qquad B_m = \begin{bmatrix} 0 & 0 & 1 & 0 \\ 0 & 0 & 0 & 1 \\ -\omega_n^2 & 0 & 0 & 0 \\ 0 & -\omega_n^2 & 0 & 0 \end{bmatrix}, \qquad C_m = \begin{bmatrix} \alpha I_2 & I_2 \end{bmatrix}$$

with

$$x_m = \begin{bmatrix} x_{r_m} \\ \dot{x}_{r_m} \end{bmatrix} \in \mathbb{R}^4, \qquad u_m = \begin{bmatrix} x_{r_d} \\ \dot{x}_{r_d} \end{bmatrix} \in \mathbb{R}^4,$$

where $x_{r_d}, \dot{x}_{r_d} \in \mathbb{R}^2$ denote the desired Cartesian position and velocity vectors as commanded by the user (i.e. user commands), respectively, which correspond to a 12.6 m × 12.6 m square trajectory. Aside from the scaling parameter which is assumed to be known, the ideal model is not based on any modeling of the plant, and was designed with $\omega_n = 10$ rad/s, $\zeta = 0.9$, and $\alpha = 0.5$. The control parameters of the DSAC composite control algorithm were determined as follows

$$\Gamma_{Pe} = 15I_2, \qquad \Gamma_{Ie} = 50I_2, \qquad \Gamma_{Px} = \Gamma_{Pu} = 0.1I_4, \qquad \Gamma_{Ix} = \Gamma_{Iu} = 0.2I_4$$

$$\sigma_e = 0.1I_2, \qquad \sigma_x = \sigma_u = \mathrm{diag}\{0.9 \quad 0.9 \quad 0.4 \quad 0.4\}, \qquad K_v = 120I_2$$

and the control parameters of the DMSAC composite controller were selected as follows

$$\Gamma_{Pe} = 15I_2, \qquad \Gamma_{Ie} = 35I_2, \qquad \sigma_e = 0.03I_2, \qquad K_v = 35I_2$$

The integral structure of the adaptive integral gains is computed online using a standard Tustin algorithm, and all integral gains were initialized to zero. Note that the control parameters were selected to provide satisfactory tracking performance along each side of the 12.6 m × 12.6 m square trajectory, with acceptable transient response at the corners when applied to the two-link flexible-joint robot modeled with the nominal linear joint stiffness dynamics representation described in Sec. II, and with physical characteristics described above. Also, the values of the selected σ-terms are relatively small, since they are only to prevent the integral adaptive gains from reaching excessively high values, or diverging in time.

Results for the DMSAC and the DSAC control laws are shown in Figs. 3 to 5, and in Figs. 6 to 10, respectively. As shown in these figures, while both controllers trajectory exhibits minimal overshoots at each direction change, with rapid settling to a steady-state along each side of the trajectory, the DSAC composite control strategy provides improved tracking results, when compared to the DMSAC composite controller. This is demonstrated in Figs. 3 and 6, where the DMSAC control strategy exhibits greater positioning overshoots; 0.117 m, 0.112 m and 0.104 m, in comparison with 0.082 m, 0.079 m and 0.079 m for the DSAC control law, at the first, second and third direction change, respectively.

The corresponding time-varying control gains, shown in Fig. 5 and Figs. 8-10, for both controller respectively, increase sharply when the end-effector reaches each corner of the square trajectory, thus adapting the control laws to reduce tracking errors and positioning +overshoots. It is also important to note that as observed in this figure, the adaptation rates (i.e. the rates of change of the adaptive gains) at each direction switch are large. These high adaptation rates ensure that the required gains are provided at the correct time, with peaks occurring only at the corners of the square trajectory. In other words, fast adaptation rates allow the controller to use low gains, and to increase them only when necessary.

To validate the robustness to parametric uncertainties, the same DMSAC and DSAC composite controllers tuned for the nominal robot manipulator were applied to the uncertain linear joint stiffness robot model, which is defined by significantly lower joint stiffness coefficients, i.e. with $k_1 = k_2 = 200$ N·m/rad. The results are provided in Figs. 11 to 18. Both composite control methodologies achieved similar tracking performance in terms of positioning errors; 0.124 m, 0.126 m and 0.121 m for the DMSAC strategy, compared with 0.127 m, 0.129 m and 0.123 m for the DSAC strategy. However, with the DSAC approach, the settling time between two direction changes is larger, as shown in Fig. 15. This can be explained by the larger control inputs associated with the DSAC strategy, due to the introduction of additional feedforward control terms in the control structure. Indeed, these terms increase the overall control effort, as required to improve the tracking performance. However, this makes the DSAC controller more sensitive to sudden changes in the desired trajectory, which in turn results in increased oscillations and settling times, as demonstrated by the obtained results. The same behavior than that obtained for the nominal case is observed in the control gains adaptation history, that is, with large adaptation rates at the corners of the trajectory, as illustrated in Fig. 13 and Figs. 16 to 18.

Finally, to validate the performance of the proposed controllers to dynamics modeling errors, both adaptive control schemes were applied to a nonlinear joint stiffness dynamics model which includes friction torques, nonlinear time-varying joint stiffness matrix, soft-windup effect, and inertial cross-coupling between joint and motor accelerations.[8] Again, the controllers were not re-tuned for this case. Both adaptive control strategies provide a

stable closed-loop behavior, yet the trajectory obtained with the DSAC control law demonstrates improved tracking results compared to the DMSAC approach, especially along each side of the trajectory, shown in Figs. 19 and 22.

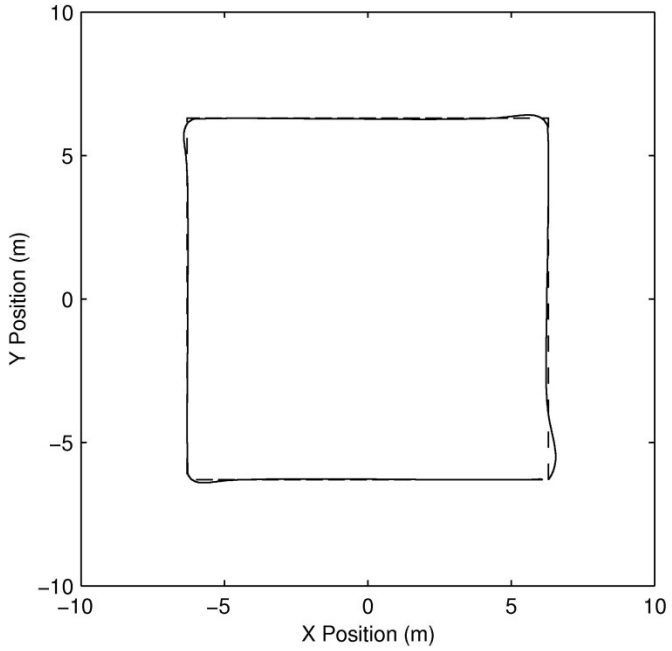

Fig. 3 Trajectory tracking results obtained with the DMSAC composite controller applied to the nominal linear joint stiffness manipulator ($k = 500I_2$ N·m). The dashed line corresponds to the desired end-effector position $x_{rd}(t)$, and the solid line corresponds to the actual end-effector position $x_r(t)$.

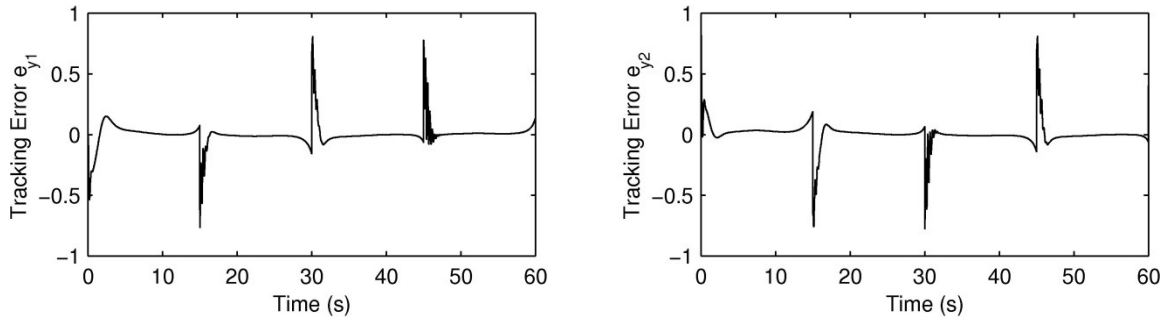

Fig. 4 Trajectory tracking errors $e_y(t) = y_m(t) - y(t)$ obtained with the DMSAC composite controller, nominal linear joint stiffness manipulator ($k = 500I_2$ N·m).

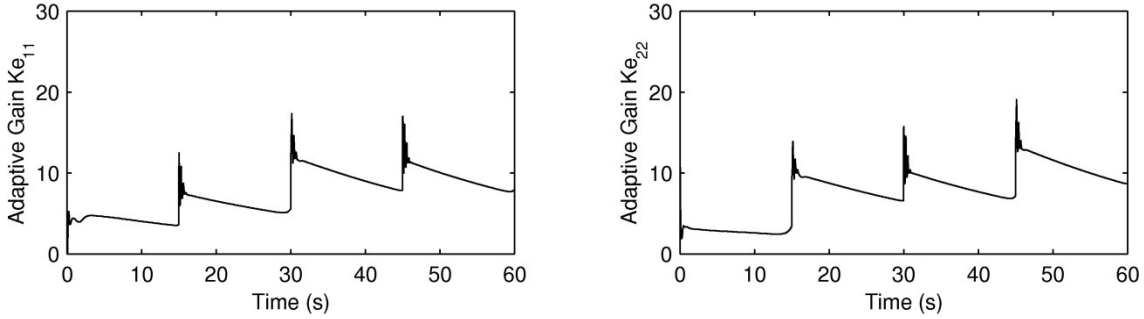

Fig. 5 Adaptation history of the DMSAC composite controller gains K_e, nominal linear joint stiffness manipulator ($k = 500I_2$ N·m).

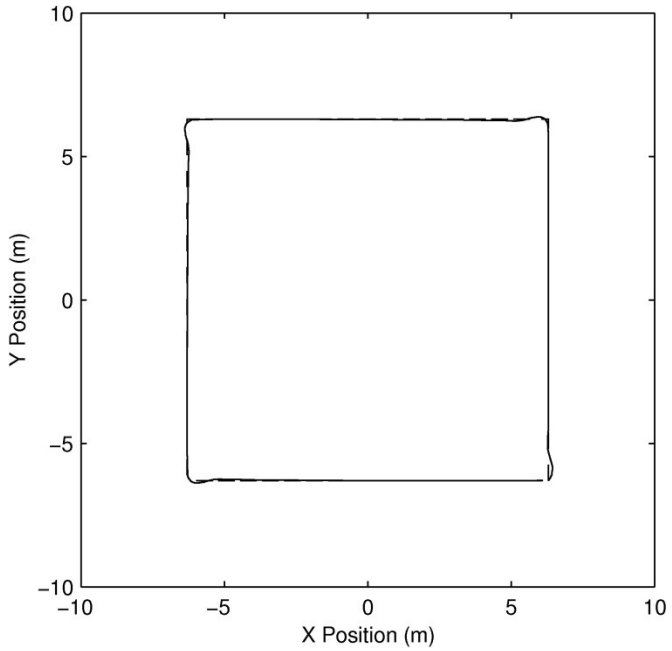

Fig. 6 Trajectory tracking results obtained with the DSAC composite controller applied to the nominal linear joint stiffness manipulator ($k = 500I_2$ N·m). The dashed line corresponds to the desired end-effector position $x_{rd}(t)$, and the solid line corresponds to the actual end-effector position $x_r(t)$.

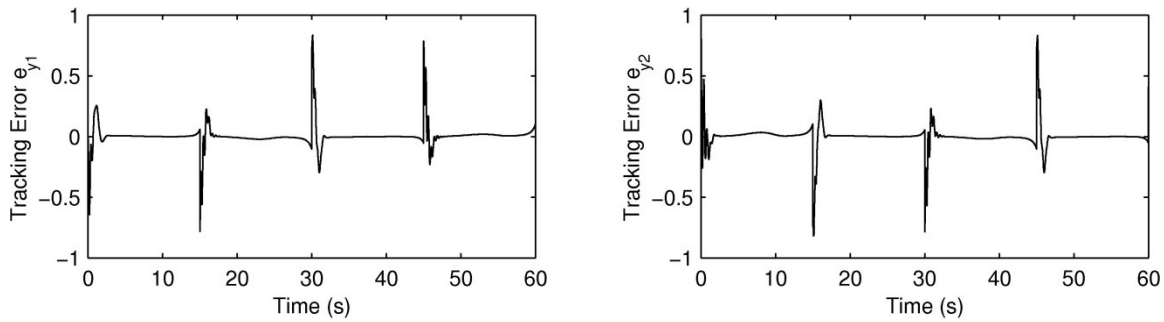

Fig. 7 Trajectory tracking errors $e_y(t) = y_m(t) - y(t)$ obtained with the DSAC composite controller, nominal linear joint stiffness manipulator ($k = 500I_2$ N·m).

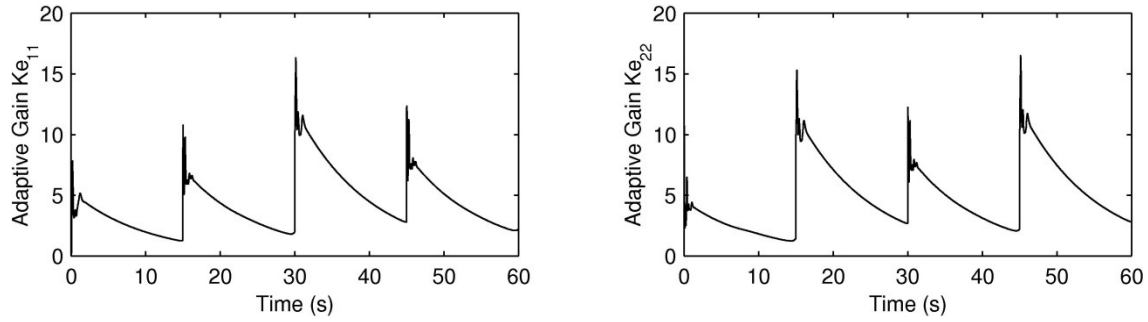

Fig. 8 Adaptation history of the DSAC composite controller gains K_e, nominal linear joint stiffness manipulator ($k = 500I_2$ N·m).

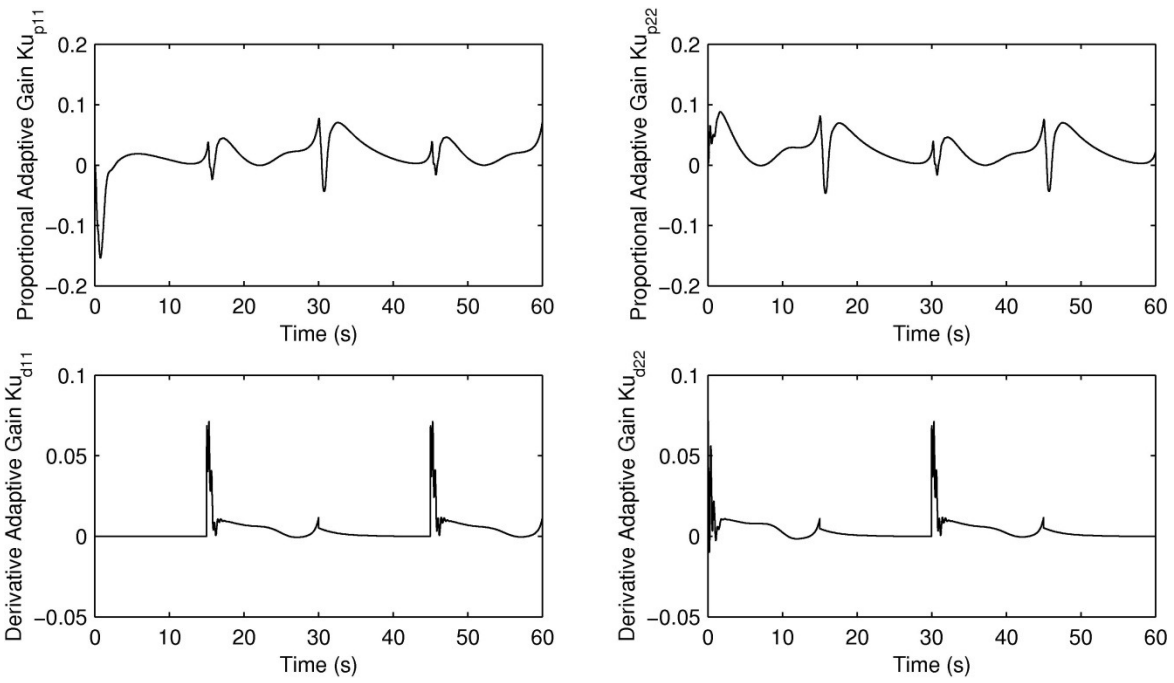

Fig. 9 Adaptation history of the DSAC composite controller gains K_u, nominal linear joint stiffness manipulator ($k = 500\boldsymbol{I}_2$ N·m).

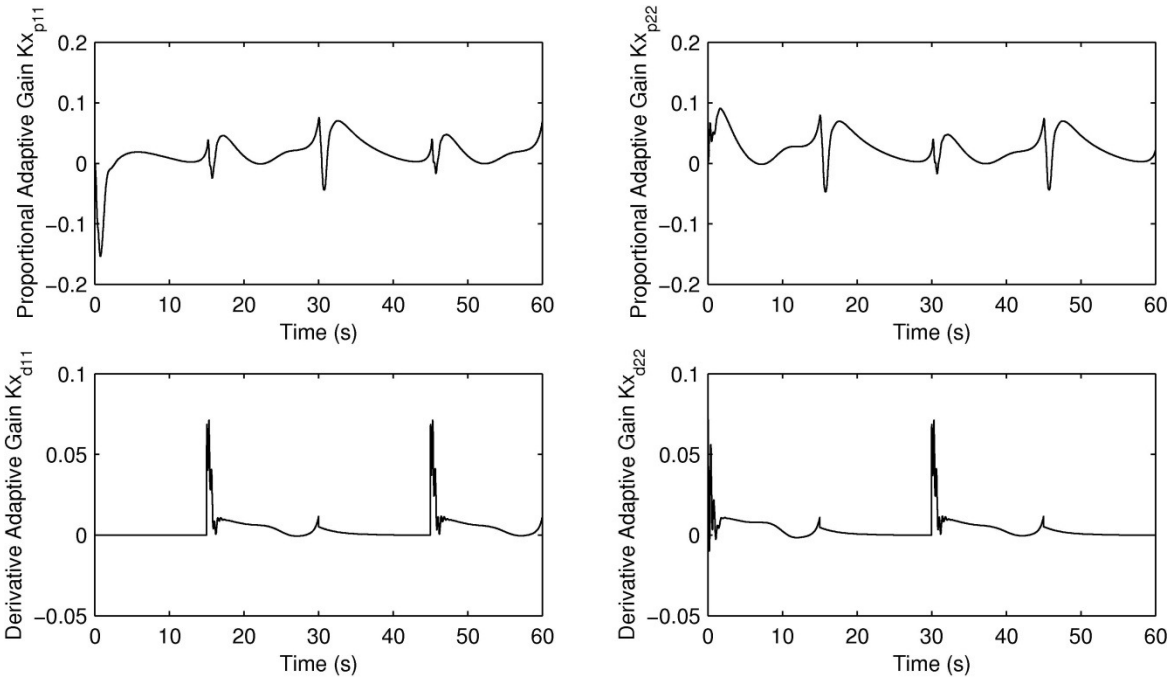

Fig. 10 Adaptation history of the DSAC composite controller gains K_x, nominal linear joint stiffness manipulator ($k = 500\boldsymbol{I}_2$ N·m).

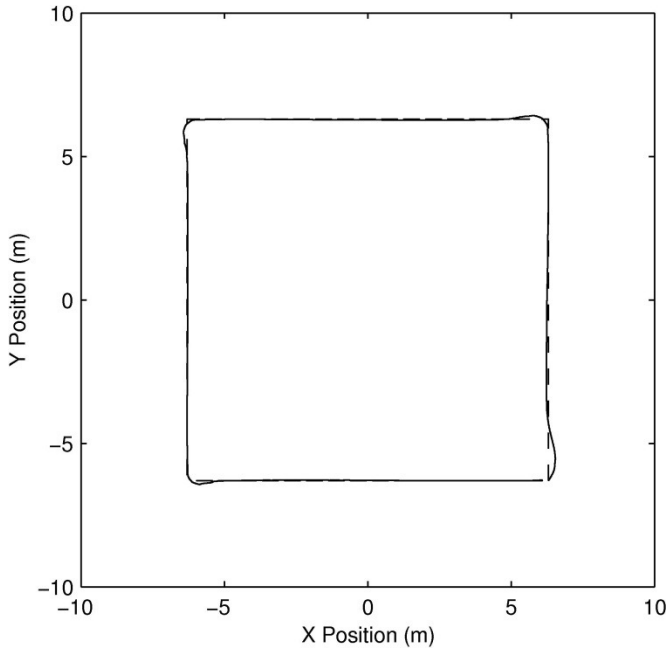

Fig. 11 Trajectory tracking results obtained with the DMSAC composite controller applied to the uncertain linear joint stiffness manipulator ($k = 200I_2$ N·m). The dashed line corresponds to the desired end-effector position $x_{rd}(t)$, and the solid line corresponds to the actual end-effector position $x_r(t)$.

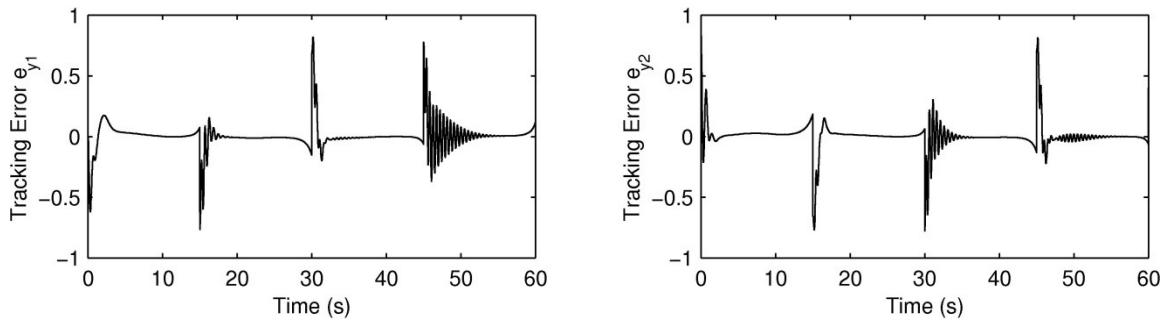

Fig. 12 Trajectory tracking errors $e_y(t) = y_m(t) - y(t)$ obtained with the DMSAC composite controller, uncertain linear joint stiffness manipulator ($k = 200I_2$ N·m).

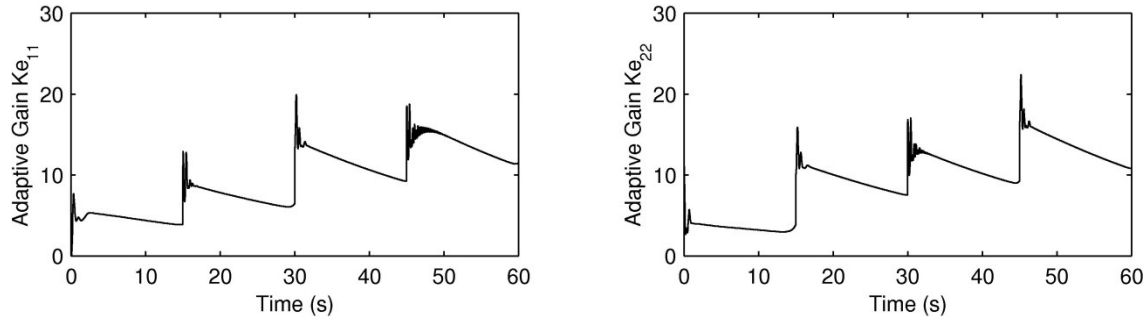

Fig. 13 Adaptation history of the DMSAC composite controller gains K_e, uncertain linear joint stiffness manipulator ($k = 200I_2$ N·m).

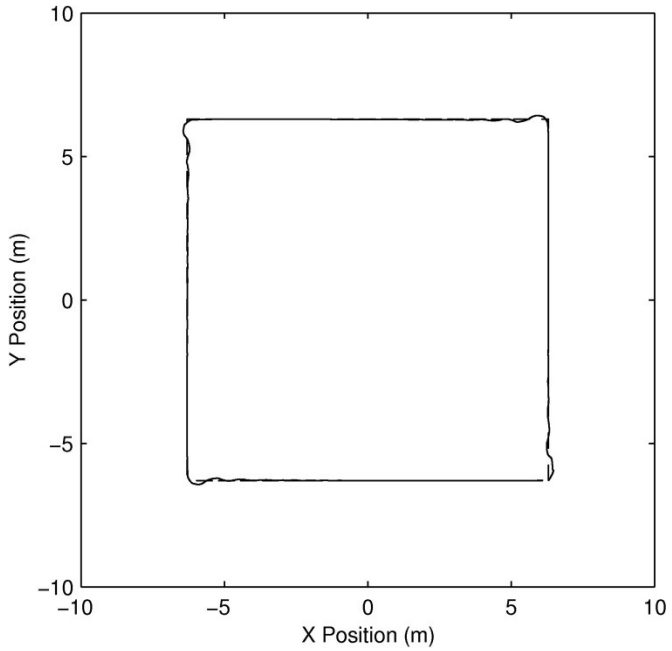

Fig. 14 Trajectory tracking results obtained with the DSAC composite controller applied to the uncertain linear joint stiffness manipulator ($k = 200I_2$ N·m). The dashed line corresponds to the desired end-effector position $x_{rd}(t)$, and the solid line corresponds to the actual end-effector position $x_r(t)$.

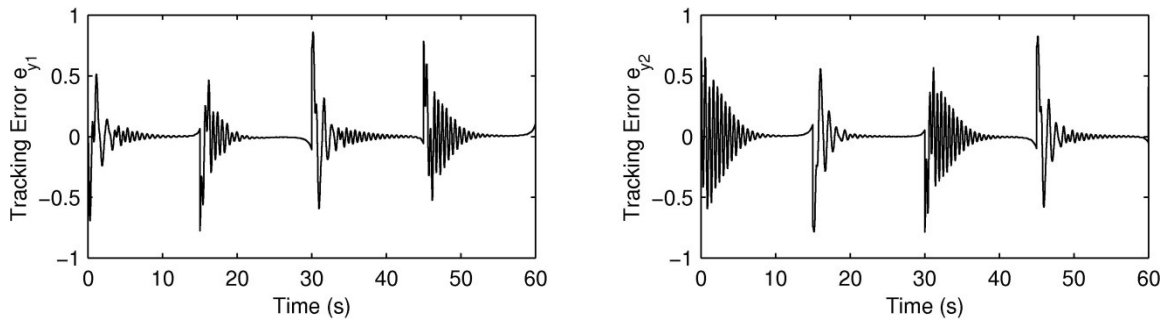

Fig. 15 Trajectory tracking errors $e_y(t) = y_m(t) - y(t)$ obtained with the DSAC composite controller, uncertain linear joint stiffness manipulator ($k = 200I_2$ N·m).

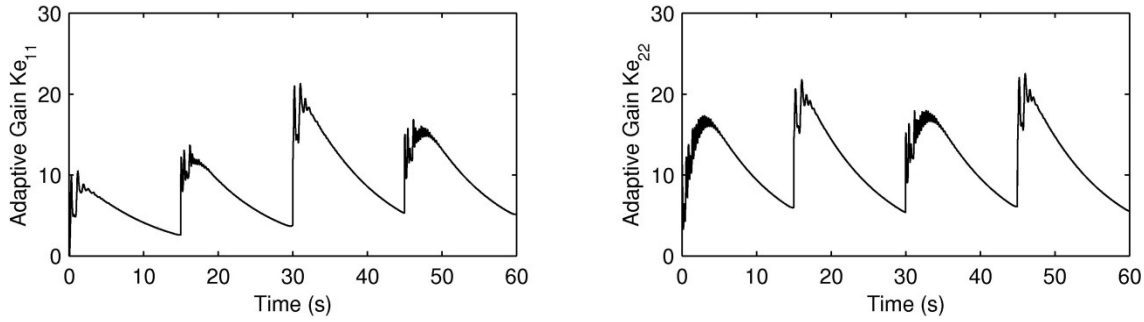

Fig. 16 Adaptation history of the DSAC composite controller gains K_e, uncertain linear joint stiffness manipulator ($k = 200I_2$ N·m).

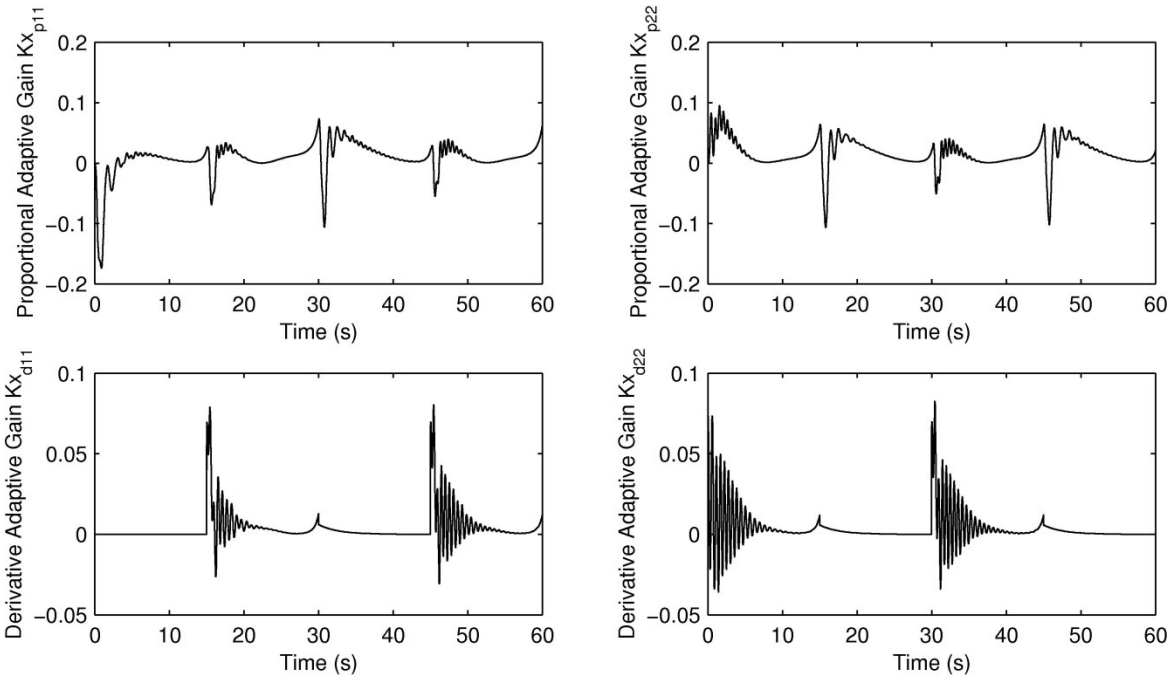

Fig. 17 Adaptation history of the DSAC composite controller gains K_x, uncertain linear joint stiffness manipulator (k = $200I_2$ N·m). (kx)

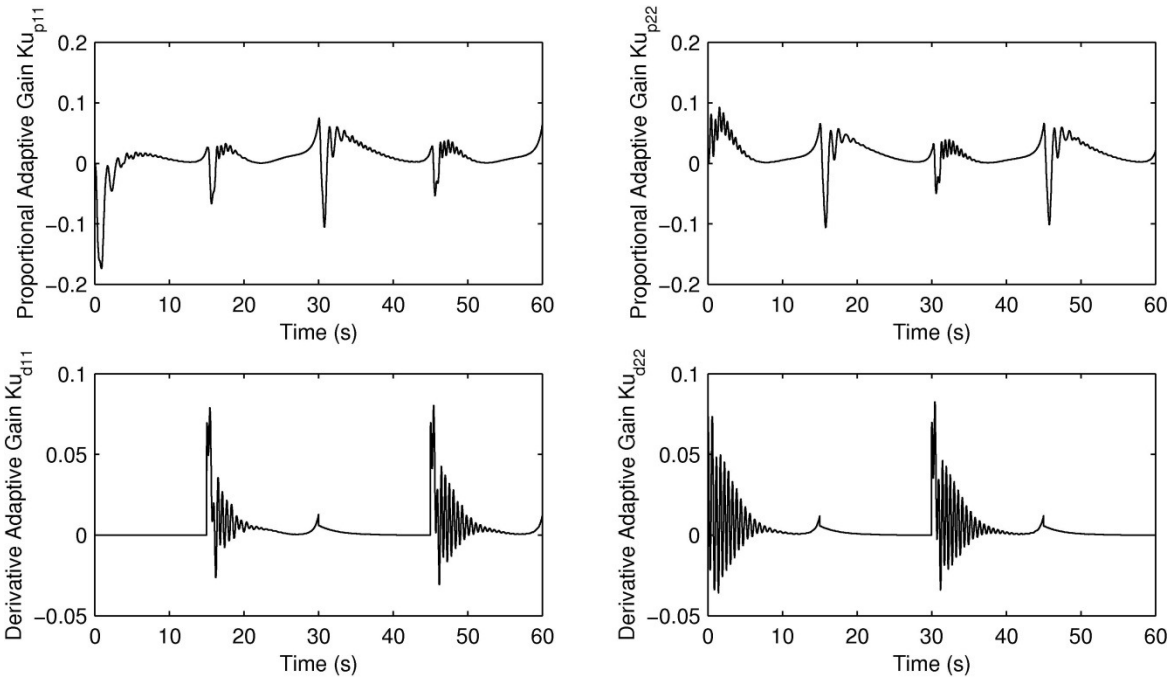

Fig. 18 Adaptation history of the DSAC composite controller gains K_u, uncertain linear joint stiffness manipulator (k = $200I_2$ N·m).

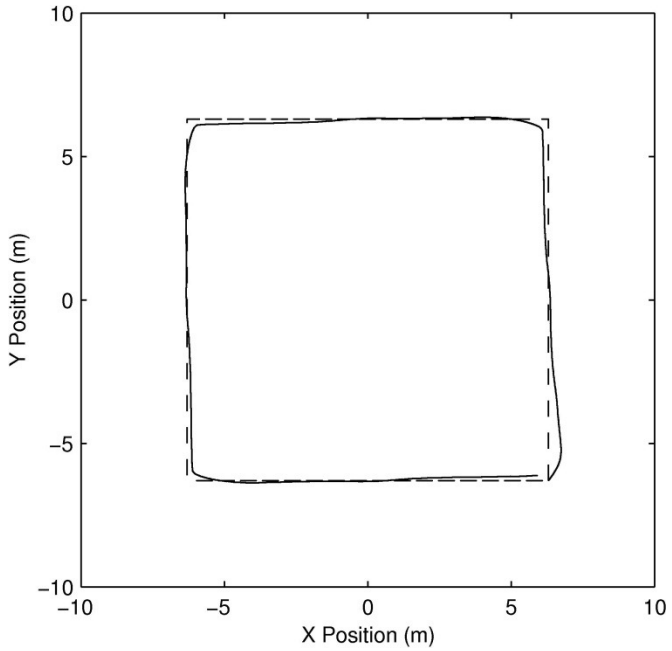

Fig. 19 Trajectory tracking results obtained with the DMSAC composite controller applied to the nonlinear joint stiffness manipulator. The dashed line corresponds to the desired end-effector position $x_{rd}(t)$, and the solid line corresponds to the actual end-effector position $x_r(t)$.

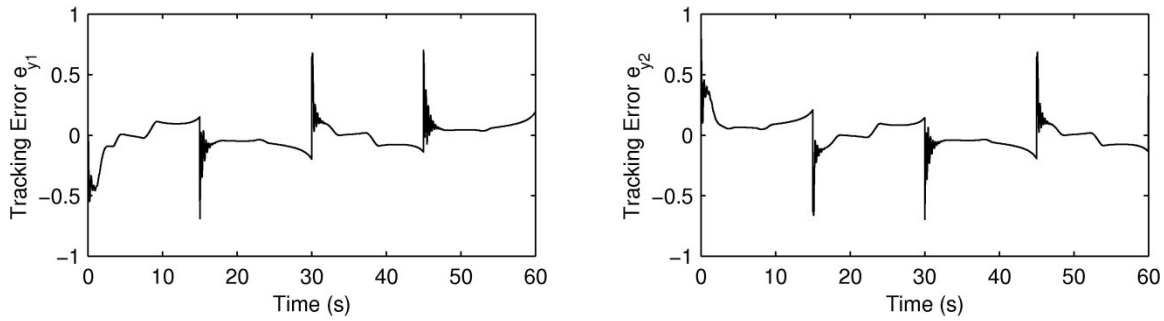

Fig. 20 Trajectory tracking errors $e_y(t) = y_m(t) - y(t)$ obtained with the DMSAC composite controller, nonlinear joint stiffness manipulator.

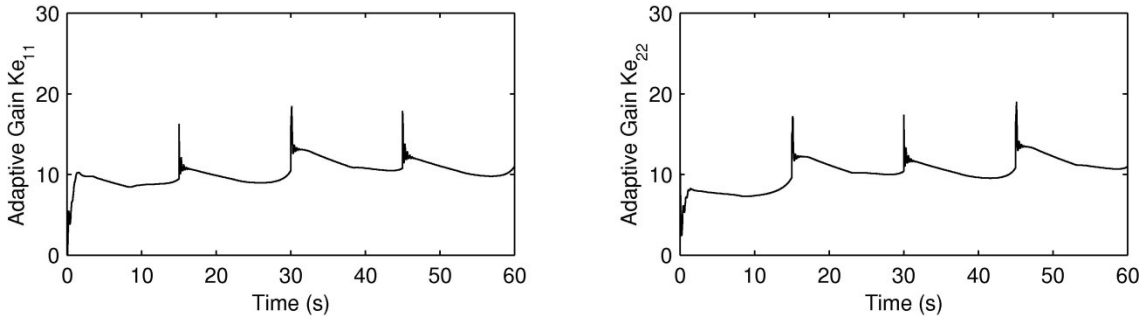

Fig. 21 Adaptation history of the DMSAC composite controller gains K_e, nonlinear joint stiffness manipulator.

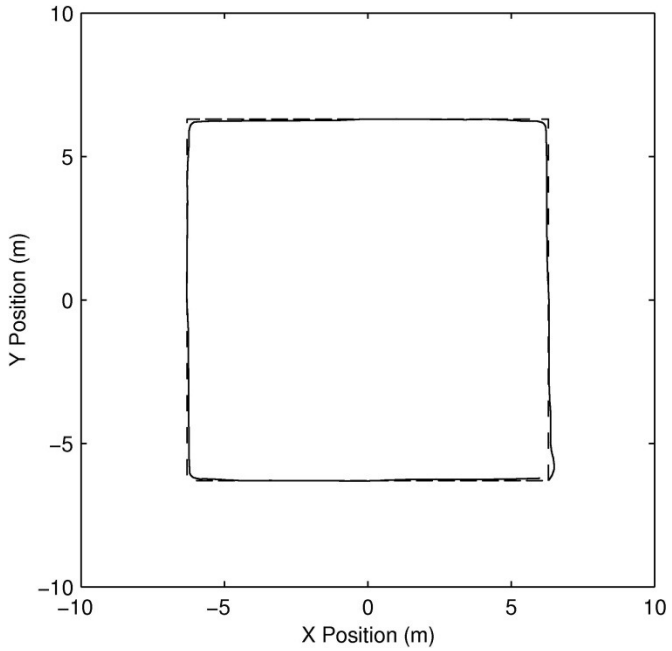

Fig. 22 Trajectory tracking results obtained with the DSAC composite controller applied to the nonlinear joint stiffness manipulator. The dashed line corresponds to the desired end-effector position $x_{rd}(t)$, and the solid line corresponds to the actual end-effector position $x_r(t)$.

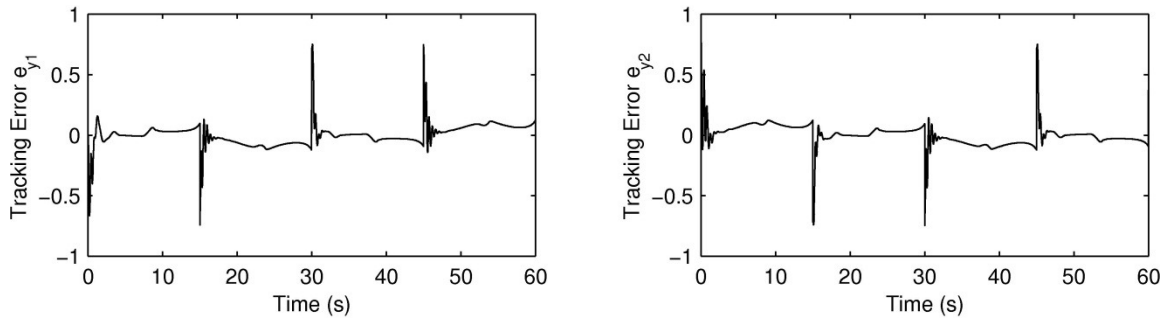

Fig. 23 Trajectory tracking errors $e_y(t) = y_m(t) - y(t)$ obtained with the DSAC composite controller, nonlinear joint stiffness manipulator.

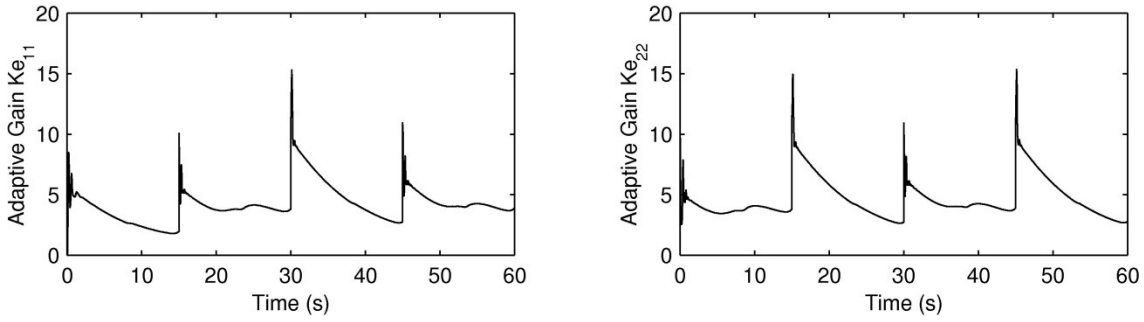

Fig. 24 Adaptation history of the DSAC composite controller gains K_e, nonlinear joint stiffness manipulator.

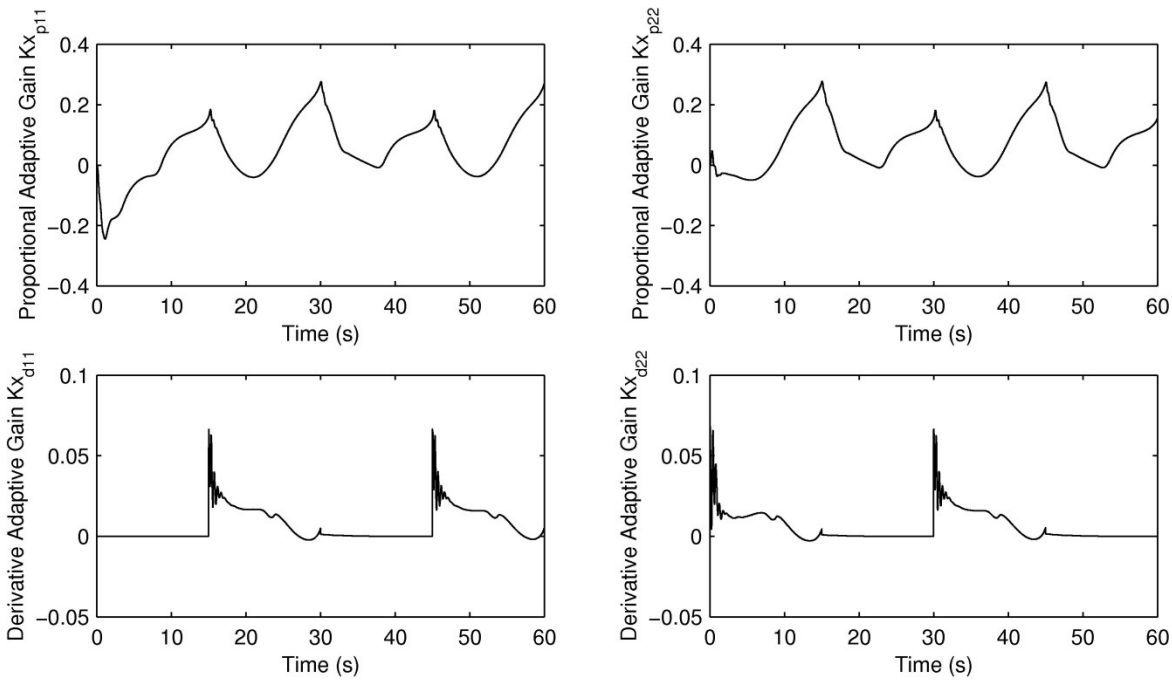

Fig. 25 Adaptation history of the DSAC composite controller gains K_x, nonlinear joint stiffness manipulator.

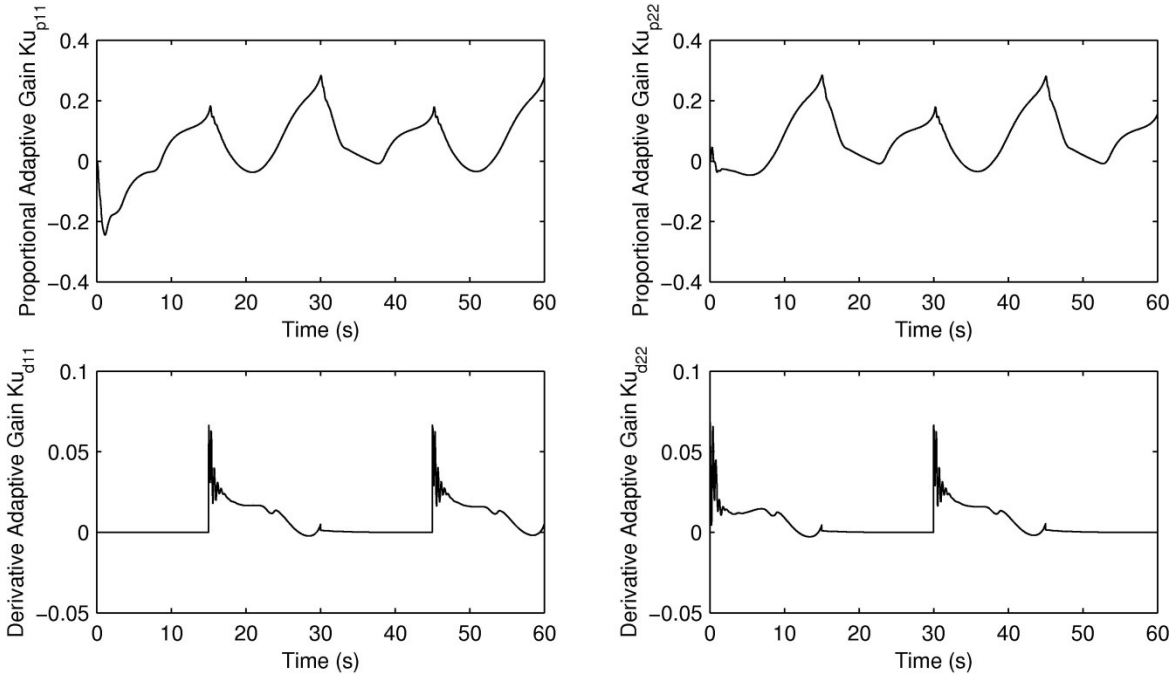

Fig. 26 Adaptation history of the DSAC composite controller gains K_u, nonlinear joint stiffness manipulator.

VIII. Conclusion

This paper addressed the problem of adaptive trajectory tracking control of robot manipulators that exhibit elastic vibrations in their joints and are subject to parametric uncertainties and modeling errors. It was shown that a flexible-joint manipulator with a scaled-position-plus-velocity feedback signal is almost strictly passive, enabling the use of nonlinear adaptive control schemes (e.g. simple adaptive control-based methodologies), while guaranteeing the closed-loop stability of the quasi-steady state subsystem. Two new direct adaptive control schemes designed to stabilize the rigid manipulator dynamics, and a simple linear control law to improve damping of vibrations at the joints were proposed. The overall stability of the flexible system is guaranteed by invoking Tychonov's theorem. Numerical simulations revealed that both control strategies are efficient at tracking a desired trajectory, regardless of parametric uncertainties and dynamics modeling errors.

Although similar ideas to those presented in Refs. 8 and 9 are used, the present work is distinctly different. First, although almost strictly passivity-based arguments are used in Ref. 8, they were not used to provide a formal proof of closed-loop stability, as this paper does, since the flexible-joint robot manipulator was modeled as a nonsquare plant. Second, the present work also develop a DSAC-based composite control strategy, which demonstrated the applicability of using additional information about the ideal model (via the use of feedforward adaptive gains) to control a flexible-joint robot manipulator.

Acknowledgments

This work was financially supported in part by the J. Y. and E. W. Wong Research Award in Mechanical/Aerospace Engineering from Carleton University, the Canadian Space Agency, the Canadian Armed Forces under the S. B. Lerner Memorial Educational Bursary, and the Natural Sciences and Engineering Research Council of Canada under the Alexander Graham Bell Canada Graduate Scholarship CGS D3-374291-2009.

References

[1]Sweet, L. M., and Good, M. C., "Re-definition of the Robot Motion Control Problem: Effects of Plant Dynamics, Drive System Constraints, and User Requirements," *23rd IEEE Conference on Decision and Control*, Inst. of Electrical and Electronics Engineers, Piscataway, NJ, Dec. 1984, pp. 724–732.

[2]van Woerkoma, P. T. L. M., and Misrab, A. K., "Robotic Manipulators in Space: A Dynamics and Control Perspective," *Acta Astronautica*, Vol. 38, No. 4-8, 1996, pp. 411–421.

[3]Ozgoli, S., and Taghirad, H. D., "A Survey on the Control of Flexible Joint Robots," *Asian Journal of Control*, Vol. 8, No. 4, 2006, pp. 332–344.

[4]Lee, J. Y., Yeon, J. S., Park, J. H., and Lee, S., "Robust Back-Stepping Control for Flexible-Joint Robot Manipulators," *IEEE International Conference on Intelligent Robots and Systems*, Inst. of Electrical and Electronics Engineers, Piscataway, NJ, 2007, pp. 183–188.

[5]Melhem, K., and Wang, W., "Global Output Tracking Control of Flexible Joint Robots via Factorization of the Manipulator Mass Matrix," *IEEE Transaction on Robotics*, Vol. 25, No. 2, 2009, pp. 428–437.

[6]Consolini, L., Gereli, O., Bianco, C. G. L., and Piazzi, A., "Minimum-Time Control of Flexible Joints with Input and Output Constraints," *IEEE International Conference on Robotics and Automation*, Inst. of Electrical and Electronics Engineers, Piscataway, NJ, 2007, pp. 3811–3816.

[7]Tomei, P., "Tracking Control of Flexible Joint Robots with Uncertain Parameters and Disturbances," *IEEE Transactions on Automatic Control*, Vol. 39, No. 5, 1994, pp. 1067–1072.

[8]Ulrich, S., Sasiadek, J. Z., and Barkana, I., "Modeling and Direct Adaptive Control of a Flexible-Joint Manipulator," *Journal of Guidance, Control, and Dynamics*, Vol. 35, No. 1, 2012, pp. 25–39.

[9]Ulrich, S. and Sasiadek, J. Z., "Direct Fuzzy Adaptive Control of a Manipulator with Elastic Joints," *Journal of Guidance, Control, and Dynamics*, Vol. 36, No. 1, 2013, pp. 311–319.

[10]Ulrich, S., "Direct Adaptive Control Methodologies for Flexible-Joint Space Robotic Manipulators with Uncertainties and Modeling Errors", Ph.D. Thesis, Department of Mechanical and Aerospace Engineering, Carleton University, Canada, August 2012.

[11]Ulrich, S., Sasiadek, J. Z., and Barkana, I., "On a New Class of Direct Adaptive Output Feedback Controllers for Nonlinear Square Systems," *IEEE Conference on Decision and Control*, Inst. of Electrical and Electronics Engineers, Piscataway, NJ, Dec 2012, pp. 4139–4144.

[12]Barkana, I. "Output Feedback Stabilizability and Passivity in Nonstationary and Nonlinear Systems," *International Journal of Adaptive Control and Signal Processing*, Vol. 24, No. 7, 2010, pp. 568–591.

[13]Spong, M. W., "Modeling and Control of Elastic Joint Robots," *Journal of Dynamic Systems, Measurement and Control*, Vol. 109, No. 4, 1987, pp. 310–319.

[14]Spong, M. W., Hutchinson, S., and Vidyasagar, M., *Robot Modeling and Control*, Wiley, New York, 2006, p.85.

[15]Kaufman, H., Barkana, I., and Sobel, K., *Direct Adaptive Control Algorithms: Theory and Applications,* 2nd ed., Communications and Control Engineering Series, New York, NY: Springer, 1997, pp. 42–45, 55–55.

[16]Ulrich, S., and de Lafontaine, J., "Autonomous Atmospheric Entry on Mars: Performance Improvement using a Novel Adaptive Control Algorithm," *The Journal of the Astronautical Sciences*, Vol. 55, No. 4, 2007, pp. 431–449.
[17]Barkana, I., and Kaufman, H., "Global Stability and Performance of an Adaptive Control Algorithm," *International Journal of Control*, Vol. 46, No. 6, 1985, pp. 1491–1505.
[18]Barkana, I., "Is there a Simple and Robust Adaptive Control? " *53 rd Israel Annual Conference on Aerospace Sciences*, Tel-Aviv & Haifa, Israel, March 2013.
[19]LaSalle, J., "Stability of Non-Autonomous Systems," *Nonlinear Analysis: Theory, Methods, and Applications*, Vol. 1, No. 1, 1981, pp. 83–90.
[20]Ioannou, P. A., and Kokotovic, P., *Adaptive Systems with Reduced Models*, New York, NY: Springer-Verlag, 1983.
[21]Khalil, H. K., *Nonlinear Systems*, Prentice Hall, 3rd ed., 2002.
[22]Spong, M. W., "Adaptive Control of Flexible Joint Manipulators: Comments on Two Papers,"*Automatica*, Vol. 31, No. 4, 1995, pp. 585–590.
[23]Readman, M. C., *Flexible Joint Robots*, Mechatronics, CRC Press, 1994, p. 4.
[24]Cao, Y., and de Silva, C.W., "Dynamic Modeling and Neural-Network Adaptive Control of a Deployable Manipulator System," *Journal of Guidance, Control, and Dynamics*, Vol. 29, No. 1, 2006, pp. 192–194.